

## Atmospheric Aerosols and Air Quality in the 2022 Dry Season in Huancayo-Perú

*Aerossóis Atmosféricos e Qualidade do Ar na Estação Seca de 2022 em Huancayo-Perú*

Roberto Angeles Vasquez<sup>1</sup> , Julio Miguel Angeles Suazo<sup>2</sup> , Hugo Abi Karam<sup>3</sup> , Jose Luis Flores Rojas<sup>4</sup> , Luis Suarez Salas<sup>4</sup> , Carmencita Lavado-Meza<sup>5</sup> , Nataly Angeles Suazo<sup>6</sup> , Fernando Boza Ccora<sup>1</sup> , Leonel De la Cruz-Cerron<sup>7</sup> , Rosa Zarate Quiñones<sup>8</sup> 

<sup>1</sup>Universidad Nacional del Centro del Perú, Facultad de Ingeniería Civil, Huancayo, Perú

<sup>2</sup>Universidad Nacional Autónoma de Tayacaja Daniel Hernández Morillo, Facultad de Ingeniería Forestal y Ambiental, Pampas, Perú

<sup>3</sup>Universidade Federal do Rio de Janeiro, Instituto de Geociências, Departamento de Meteorologia, Rio de Janeiro, RJ, Brasil

<sup>4</sup>Instituto Geofísico del Perú, Ate, Perú

<sup>5</sup>Universidad Nacional Intercultural de la Selva Central Juan Santos Atahualpa, Escuela Profesional de Ingeniería Ambiental, Chanchamayo, Perú

<sup>6</sup>Universidad Tecnológica del Perú, Facultad de Ingeniería de Sistemas, Lima, Perú

<sup>7</sup>Universidad Continental, Facultad de Ingeniería, Huancayo, Perú

<sup>8</sup>Universidad Nacional del Centro del Perú, Facultad de Ciencias Forestales y del Ambiente, Huancayo, Perú

E-mails: roanvas@hotmail.com; julio\_as\_1@hotmail.com; hugo@igeo.ufrj.br; jflores@igp.gob.pe; lsuarez@igp.gob.pe; clavado@uniscjsa.edu.pe; nati2643@hotmail.com; fboza@uncp.edu.pe; ldelaacruz@continental.edu.pe; rzarate@uncp.edu.pe

**Corresponding author:** Julio Angeles Suazo; julio\_as\_1@hotmail.com

### Abstract

This work presents results of Aerosol Optical Depth (AOD) and Direct Radiative Force (DRF) at the top of the atmosphere (TOA), obtained during monitoring campaigns carried out at the Huancayo Observatory of the Geophysical Institute of Peru (OH-IGP) in April and August 2022. In these campaigns, a Sun CIMEL photometer was used to measure the microphysical and optical properties of aerosols at wavelengths ranging from 340 to 1020 nm, and a low-cost Purple-air sensor to quantify the concentration of material particulate (PM), in fine and coarse modes. The AOD results indicated values in the range 0.06-0.22. The daily averages of PM<sub>2.5</sub> and PM<sub>10</sub> did not exceed Peru's current Environmental Quality Standards (50 µg/m<sup>3</sup> and 100 µg/m<sup>3</sup>). The air quality index (AQI) calculated for PM<sub>2.5</sub> and PM<sub>10</sub> was classified as good. On some days during the campaigns, the air quality was classified as moderate. These results contribute to a better understanding of the current climatic conditions of the Peruvian Altiplano.

**Keywords:** Particulate matter; Balance energy; Purple air Sensor

### Resumo

Este trabalho apresenta resultados observacionais de Profundidade Óptica de Aerossóis (AOD) e Força Radiativa Direta (DRF) no topo da atmosfera (TOA), obtidos durante campanhas de monitoramento realizadas no Observatório Huancayo do Instituto Geofísico do Peru (OH-IGP) em Abril e agosto de 2022. Nessas campanhas, um fotômetro Sun CIMEL foi usado para medir as propriedades microfísicas e ópticas de aerossóis, em comprimentos de onda variando de 340 a 1020 nm, e um sensor Purple-air de baixo custo para quantificar a concentração de material particulado (MP), nos modos fino e grosso. Os resultados de AOD indicaram valores na faixa de 0.06-0.22. As médias diárias de PM<sub>2.5</sub> e PM<sub>10</sub> não excederam os atuais Padrões de Qualidade Ambiental do Peru (50 µg/m<sup>3</sup> e 100 µg/m<sup>3</sup>). O índice de qualidade do ar (IQA) calculado para PM<sub>2.5</sub> e PM<sub>10</sub> foi classificado como bom. Em alguns dias das campanhas, a qualidade do ar foi classificada como moderada. Esses resultados contribuem para uma melhor compreensão das atuais condições climáticas do Altiplano peruano.

**Palavras-chave:** Material particulado; Balance de energia; Sensor purple air

Received: 26 December 2022; Accepted: 22 April 2024

Anu. Inst. Geociênc., 2024;47:56253

DOI: [https://doi.org/10.11137/1982-3908\\_2024\\_47\\_56253](https://doi.org/10.11137/1982-3908_2024_47_56253) 1



## 1 Introduction

The urban pollution sources are quite variable in space and time. Atmospheric aerosols cause an impact on the environment and regional and global air quality. Atmospheric aerosols play an important role in the global energy balance by scattering and absorbing the solar and terrestrial radiation (direct effect), as well as by acting as cloud condensation nuclei (indirect effect) ([Masson-Delmotte et al. 2021; IPCC 2007]). It can be derived from natural as well as anthropogenic sources especially the urban pollution which is quite variable in space and time.

Aerosols are known to affect the air quality, human health and Earth radiation budget. The direct effect due to aerosols as effect of both natural and anthropogenic on the radiation budget primarily due to scattering and absorption of radiation by aerosols and is measured in terms of watts per square meter ( $W/m^2$ ) or also known as aerosol radiative forcing (ARF) (Srivastava et al. 2012).

Aerosol particles play a vital role in global climate change, ecosystem, and human health (Habib et al. 2019; Kuttippurath & Raj 2021). To date, there has been increasing worry about the high aerosol concentration events in the atmosphere in all regions of Peru, which cause air pollution and health problems.

Ground radiometric measurements offer key information which complements that provided by satellites. A successful example of surface aerosol measurements is the global sunphotometer of red Aerosol Robotic Network (AERONET), coordinated by NASA (Holben et al. 1998). For example, Direct sun measurements with a CIMEL sunphotometer belonging to the AERONET network have been performed in the Huancayo Observatory, Peru.

The month with the maximum AOD monthly average is September, and in 2016, the absolute maximum value of 0.91 was registered. The mean AOD value for the study period is  $0.10 \pm 0.07$  and the alpha mean value is  $1.49 \pm 0.36$ , indicating presence, of small size aerosols. The aerosol size distribution revealed a bimodal character with a slight predominance of the fine mode, related to the two main types of aerosols: continental and biomass (Estevan et al. 2019).

Suazo et al. (2020) describe the results of the study of aerosol optical depth (AOD) and Direct Radiative Forcing (DRF) in Top Of Atmosphere (TOA), in the Metropolitan Huancayo Area in the months of June and July 2019, used the BF5 sensor. This instrument measured Direct, Diffuse and Global Radiation in low wavelength. The results calculated of AOD presents the value maximum that is 0.58 (11 of June) and minimum that is 0.19 (12 June).

The Angstrom coefficient presents the mean value varied from 0 to 1.8, that indicated the presence the aerosols

types biomass burning and industrial. Recorded optical properties used to estimate the direct aerosol radiative forcing (DARF) at the top of the atmosphere. The results indicates that the direct aerosol radiative forcing in Huancayo is between  $[0\ 20] W/m^2$ .

Álvarez-Tolentino and Suárez-Salas (2020) evaluated the temporal variation and source zones of PM<sub>2.5</sub> through the use of low-cost sensors installed at three sites in the city of Huancayo (August 2018 to June 2019). The results show in dry season mean of  $28.5 \pm 13 \mu g/m^3$  (2018–2019). The present research work calculate the properties aerosols atmospheric, its quality of air and radiative forcing direct in dry season 2022 in observatory of Huancayo, Perú.

## 2 Methods

### 2.1 Site Description

Meteorological and aerosol measurements are developed at the Observatory of Huancayo of the Geophysical Institute of Peru, located at the province of Chupaca that is part of the Department of Junín, Peru (Figure 1).

### 2.2 Instrument

#### 2.2.1. AERONET network

The Aerosol Robotic Network (AERONET) is a global measurement network of ground-based sun photometers supported by NASA's and other international institutions (Bedareva, Sviridenkov & Zhuravleva 2014; Holben et al. 1998), which is designed to provide long-term, continuous measurements on microphysical and optical properties of aerosols at wavelengths ranging from 340 to 1020 nm (Gobbi et al. 2007).

#### 2.2.2. The Purple Air PA-II Low-Cost PM Monitor

The PurpleAir (PA-II) sensor is a low-cost optical particle counter for PM<sub>1.0</sub> PM<sub>2.5</sub> and PM<sub>10</sub> mass concentrations in air in  $\mu g\ m^{-3}$ , incorporating a pair of Optical Particle Counter (OPC) sensors laser (Plantower Ltd., Beijing, China), together with a temperature, relative humidity and barometric pressure sensor, connected to a microcontroller equipped with a communication module of wireless network. The device records and transmits data via Wi-Fi to a cloud-based platform (Ardon-Dryer et al. 2020; Sayahi et al. 2019)

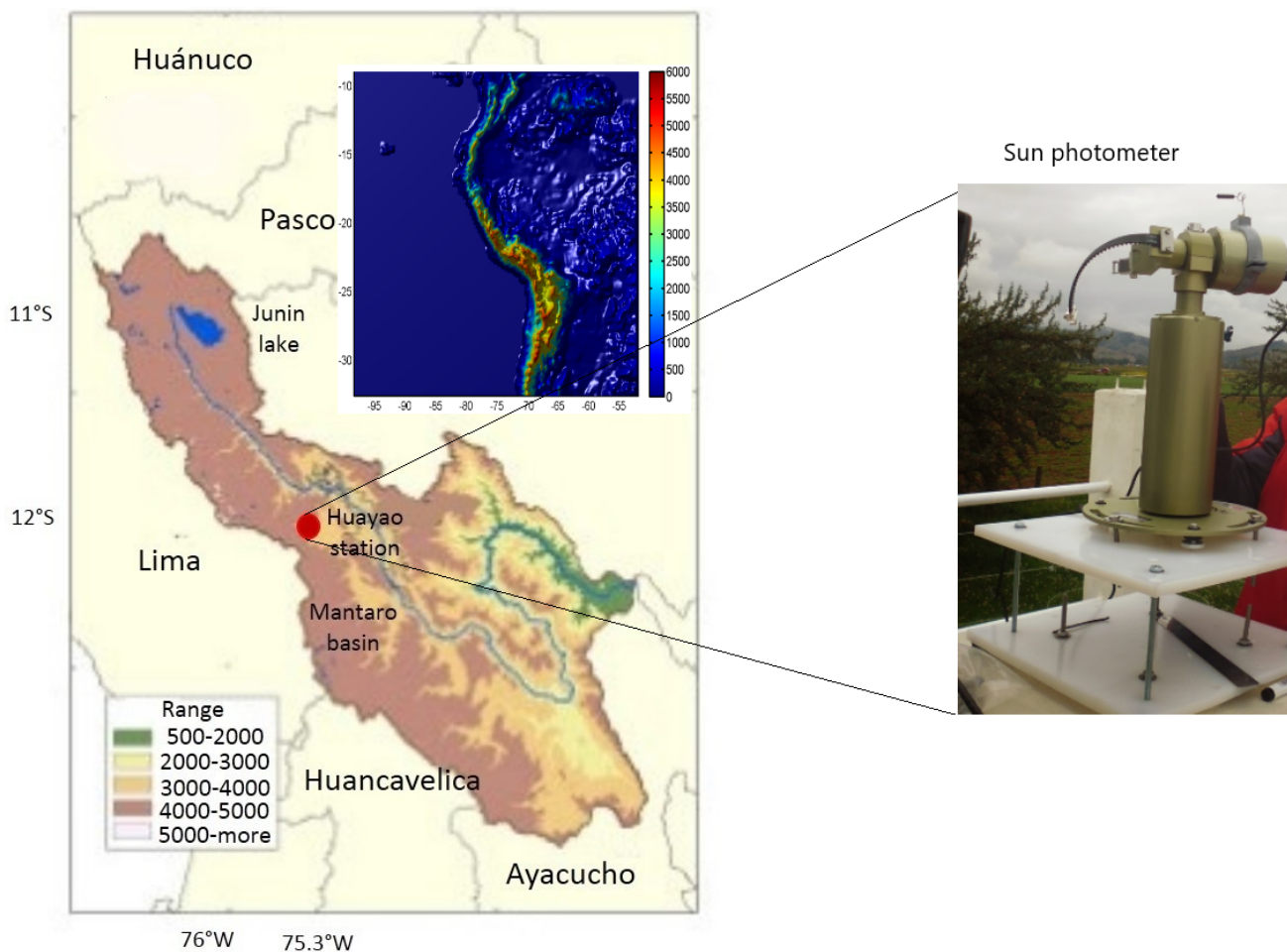


Figure 1 Location map of the Observatory of Huancayo (OH) indicated by a red circle.

### 2.3 Direct Radiative Forcing

The attenuation of aerosols during clear sky conditions is known as the ‘direct’ influence of aerosols on climate. This effect results from backscattering and absorption of radiation by the aerosol particles themselves (Charlson et al. 1992; Haywood & Boucher 2000). Although many monitoring efforts the broad range of estimates due to aerosol direct radiative forcings still remains large and an important source of uncertainty in climate models ([Masson-Delmotte et al. 2021; Forster et al. 2010).

The annual mean at the top of the atmosphere direct shortwave aerosol radiative forcing, DF, can be roughly estimated using Equation 1 and some values suggested by (Haywood & Shine 1995).

$$\Delta F = -DS_oT_{at}^2(1 - Ac)\omega\beta\tau \left( (1 - R_s)^2 - \frac{2R_s}{\beta} \left( \frac{1}{\omega} - 1 \right) \right) \quad (1)$$

where

- D is the fractional day length (0.5 to OH),

- $S_o$  is the solar constant ( $1370 \text{ Wm}^{-2}$ ),
- $T_{at}$  the atmospheric transmission (0.76),
- Ac fractional cloud cover (0.35 to OH respectively, based on the mean daily record of Cloud\_Fraction from the Moderate Resolution Imaging Spectroradiometer (MODIS) sensor for King George Island site),
- $R_s$  the surface reflectance (0.20 to OH based on the mean daily record of Effective surface reflectivity at 360 nm (%) from Ozone Monitoring Instrument (OMI) sensor),
- $\omega$ , the single scattering albedo, calculate with AERONET inversion code provides aerosol optical properties in the total atmospheric column derived from the direct and diffuse radiation measured by AERONET Cimel sun/sky-radiometer (Dubovik & King 2000; Holben et al. 2006)
- $\beta$ , the upscatter fraction (0.27, based on measurement of medium latitudes),
- $\tau$ , the aerosol optical depth.

## 2.4 Air Quality Index

To standardize and simplify the air quality assessment, the computation of the air quality index (AQI) was carried out for each pollutant, according to the Equation 2 following the recommendations of the Brazilian Ministry of Environment. Depending on the index obtained, the air quality score could be ranked with good, regular, poor, very poor, or terrible.

$$AQI = I_{ini} + \frac{I_{fin} - I_{ini}}{C_{fin} - C_{ini}} * (C - C_{ini}) \quad (2)$$

where,  $I_{ini}$  is a value that corresponds to the initial concentration of the range,  $I_{fin}$  is a value that corresponds to the final concentration of the range,  $C_{ini}$  is the initial concentration of the range in which the measured concentration is located,  $C_{fin}$  is the final concentration of the range in which the measured concentration is located and  $C$  is the measured pollutant concentration (Beringui et al. 2022, 2023).

The daily AQIs are calculated based on the 24-h average concentration for PM2.5 and PM10 the ranges of AQI values related to air quality can be classified into five classes as presented in Table 1.

**Table 1** Air quality index (AQI) range and air classification according to index values.

Class	Range	Air classification	Color identification
I	0-40	Good	green
II	41-81	Moderate	yellow
III	81-120	Poor	orange
IV	121-200	Very poor	Red
V	201-400	terrible	purple

## 3 Results

### 3.1 Aerosol Optical Depth

Also in urban cities, values of AOD vary from 0.25 to 1.7 (Castro et al. 2001), and much lower that records during biomass burning season where values can have values as high as 2.4 for the same wavelengths (Eck et al. 2003). Then, the Figure 2A, in relation to AOD in OH, presents the value maximum that is 0.24 (April) and minimum that is 0.05 (June).

Likewise, other investigations carried in Huancayo obtain the month with the maximum AOD monthly average is September, and in 2016, the absolute maximum value of 0.91 was registered. The mean AOD value for the study period is  $0.10 \pm 0.07$  and the alpha mean value is  $1.49 \pm 0.36$ , indicating presence, of small size aerosol (Estevan et al. 2019).

### 3.2 Coefficient Angstrom

Angstrom coefficient  $\alpha$  is useful to compare and characterize the wavelength dependence of AOD and columnar aerosol size distribution (Eck et al. 1999). Smaller

values represent bigger particles, for example dust. On the other hand, higher values represent smaller particles like smoke and/or burning particles (Shifrin 1995).

One way to discriminate if the aerosols are mainly composed by particles of medium – small radius, smaller than 1  $\mu\text{m}$ , or higher is to calculate the Ångström for the evaluated days. Values of  $\alpha$  that are in the range of 0.12 and 0.4 indicates the presence of particles of big size (Otero et al. 2006), as it is shown in Figure 2B from for the OH. The mean value for Angstrom coefficient ( $\alpha$ ) varied from 0.03 to 1.6 (April) that represents a low variability that can be both to instrumental and atmospheric properties.

### 3.3 Size Distribution

The aerosol volume-size distribution is derived from the irradiance measurements of the sky using the AERONET inversion algorithms (Dubovik & King 2000).

Figure 2C shows the average values of the aerosol volume-size distribution for April at August. The distribution has a bimodal character with a slight predominance of the coarse mode. The coarse mode is centered, on average, at a radius equal to 7  $\mu\text{m}$ , while the fine mode (large particles) is centered at a radius of 0.5  $\mu\text{m}$ .

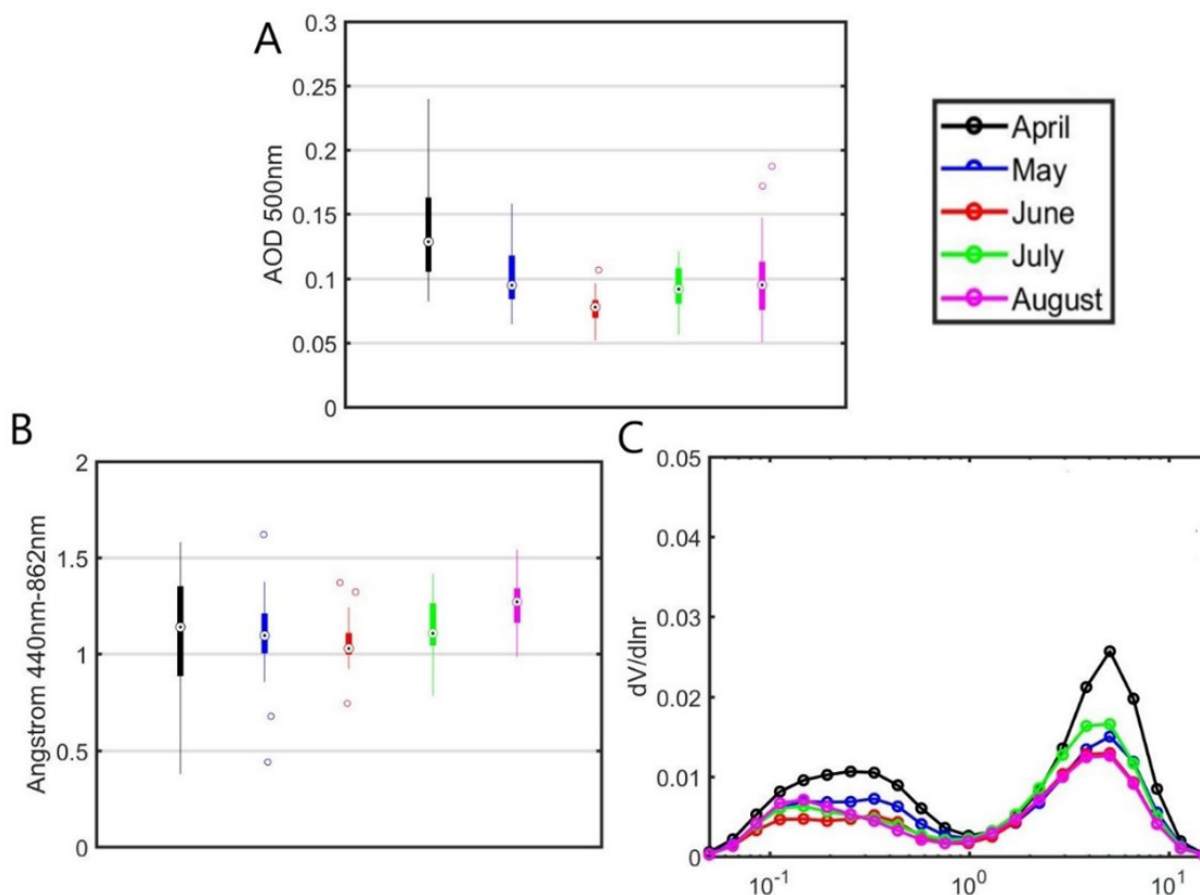


**Figure 2** Monthly variation of: A. AOD at 500 nm; B. Coefficient angstrom; C. Size distribution to OH.

Average monthly values of the aerosol volume-size distribution are shown in Figure 3. Maximum values correspond to the coarse mode, be found between the months of April and August with magnitudes higher than  $0.06 \mu\text{m}^3 \mu\text{m}^{-2}$  and correspond to the coarse mode (Figure 3A). The fact that maximum values of coarse mode appear in April and not in August attracts attention. The possible answer to this is related to the amount of aerosols suspended in the atmosphere due to scarce rains in the dry season.

### 3.4 Single Scattering Albedo

The aerosol single scattering albedo (SSA) is the most important intensive particle parameter controlling aerosol direct radiative forcing (Chýlek et al. 2000). This is a variable correlated with the radiative forcing of the Earth’s atmosphere and is defined as the amount of dispersion in relation to the total extinction in a small volume of aerosols.

Values of SSA close to 0 correspond to purely absorbing particles, while values close to unity are related to purely scattering particles (Estevan et al. 2019; Olcese, Palancar & Toselli 2014). The SSA decreases in months of July (0.84) and incremented in month of April (0.99) and August (0.97) (Figure 4A). This is due to the low rainfall and also to the fact that in the months of May to August the number of biomass fires increases (Estevan et al. 2019).

### 3.5 Concentration of Particulate Matter

Regarding the monthly variation of PM<sub>2.5</sub>, the maximum and minimum averages were recorded in the month of April ( $19 \mu\text{g}/\text{m}^3$ ) and June ( $9 \mu\text{g}/\text{m}^3$ ) respectively. Likewise, the maximum and minimum values of PM<sub>10</sub> were recorded in the month of April ( $35 \mu\text{g}/\text{m}^3$ ) and June ( $1 \mu\text{g}/\text{m}^3$ ) respectively.



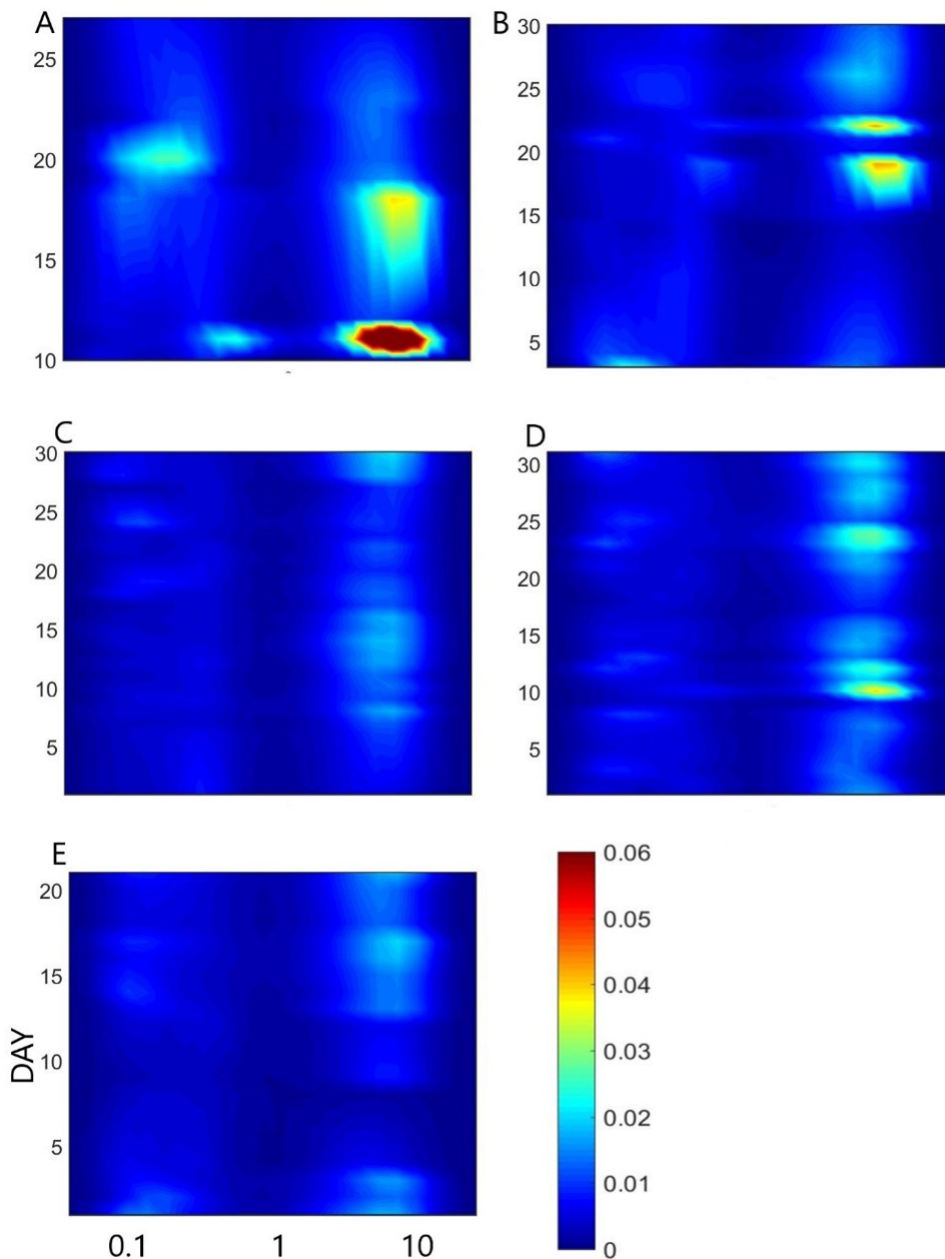


**Figure 3** Size distribution for year 2022 in: A. April; B. May; C. June; D. July; E. August.

Notwithstanding the monthly variation of PM10, the maximum and minimum averages were recorded in April ( $23 \mu\text{g}/\text{m}^3$ ) and June ( $12 \mu\text{g}/\text{m}^3$ ) respectively (Figure 5). Likewise, the maximum and minimum values of PM10 were recorded in the month of April ( $44 \mu\text{g}/\text{m}^3$ ) and June ( $2 \mu\text{g}/\text{m}^3$ ) respectively.

Comparing the daily averages of PM2.5 and PM10 with the Environmental Quality Standards of the Peruvian regulations ( $50 \mu\text{g}/\text{m}^3$  and  $100 \mu\text{g}/\text{m}^3$ ), it was determined that it was not exceeded.

### 3.6 Air Quality Index

The Air Quality Index (AQI) was calculated for PM2.5, and PM10, during April - August 2022. AQI to PM2.5 presented values lower than 40, which is classified as “good” 98% of the time (Figure 6). AQI to PM10 were also ranked as “good” in most days of the evaluated period. In a few random days, the air quality was classified as “moderate”.



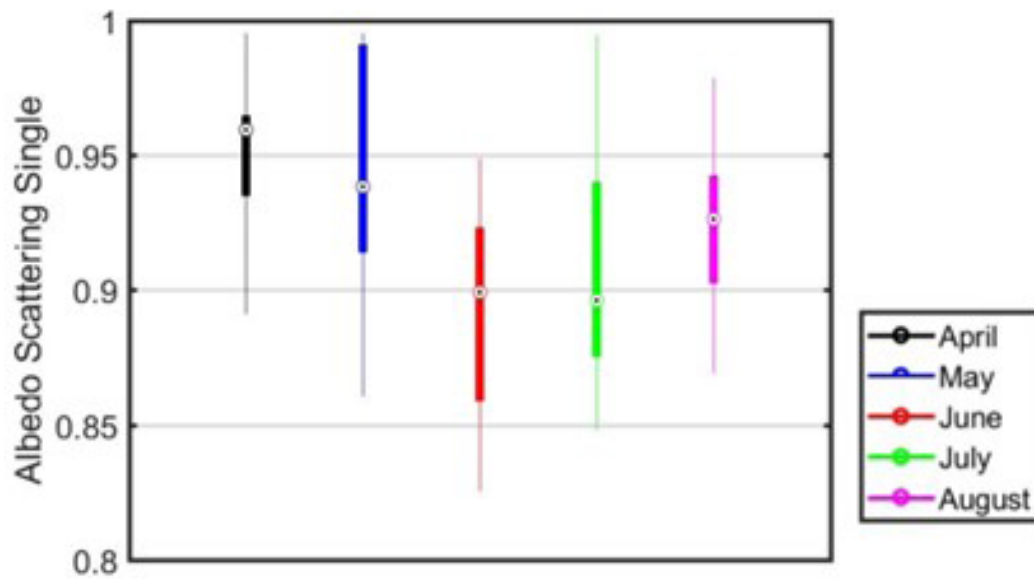


Figure 4 Scattering single Albedo to April, May, June, July and August 2022.

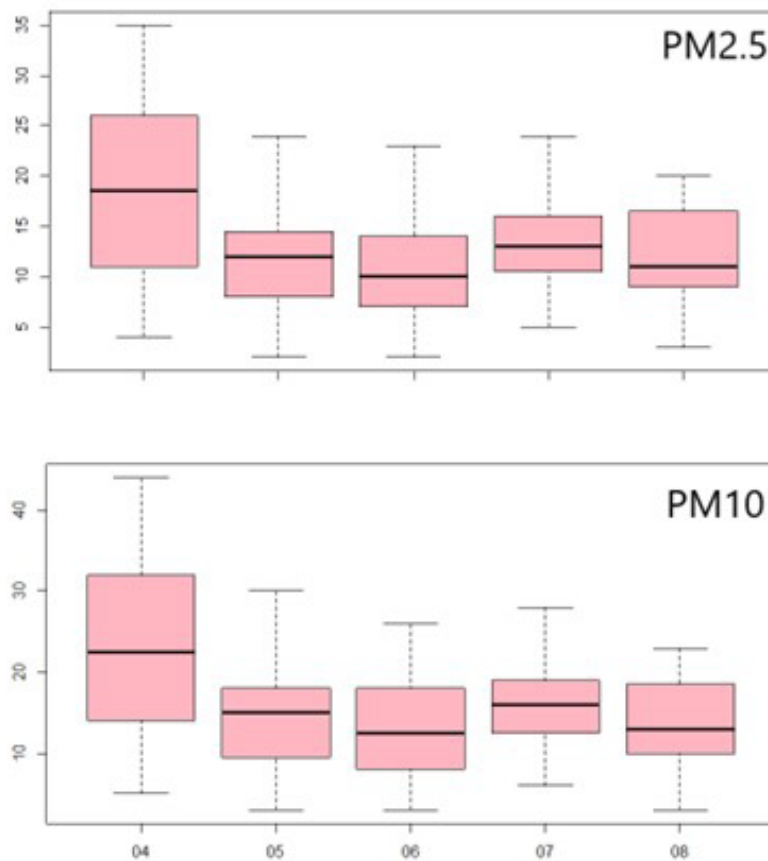


Figure 5 Boxplot of concentrations of PM2.5 and PM10 monthly to 2022.

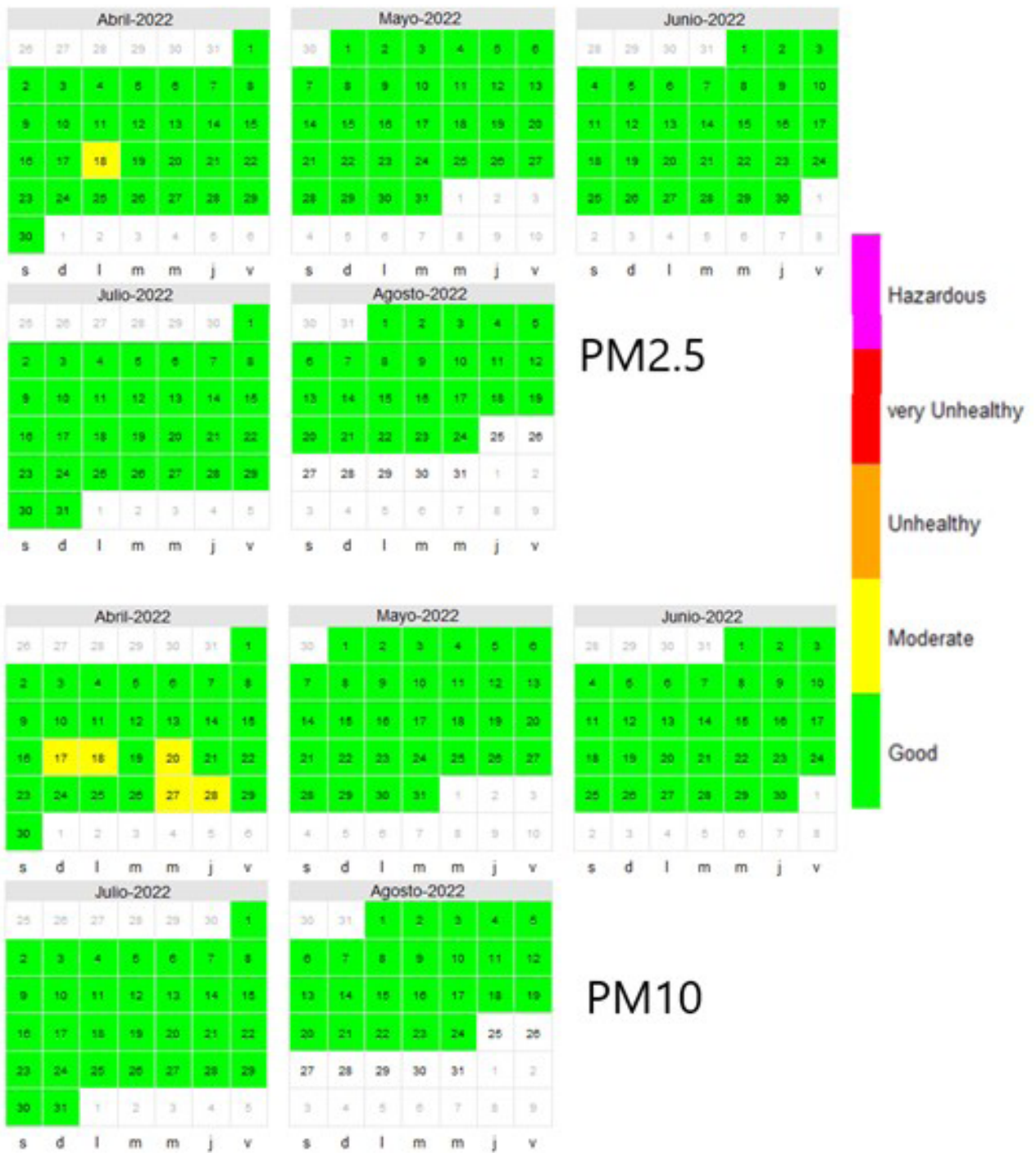


Figure 6 Index quality air of PM2.5 and PM10 during April–August 2022.



### 3.7 Aerosol Direct Radiative Forcing

The TOA Aerosol Direct Radiative Forcing (ADRF) is strongly dependent of AOD ( $\tau_a$ ) and of single scattering albedo (SSA,  $\omega_0$ ), that it is a measure of scattering and absorption processes of solar light caused by aerosols becoming a key variable for ADRF calculate.

Comparing the forcing estimates with AOD values, we find that the radiative forcing is primarily governed by

the magnitude of AODs which varied from a low value of 0.06 to high values above 0.22 at 0.5  $\mu\text{m}$ .

For evaluating and estimating the ADRF it was used the median of AOD (at 500 nm) as it is the most representative value due to this non-parametric distribution. Our estimation based on the Equation 1 the direct aerosol radiative forcing is between  $[-0.5 \ 2.5] \text{ W/m}^2$  Also, the Figure 7 shows minimum values of ADRF product of maximum values of AOD and SSA.

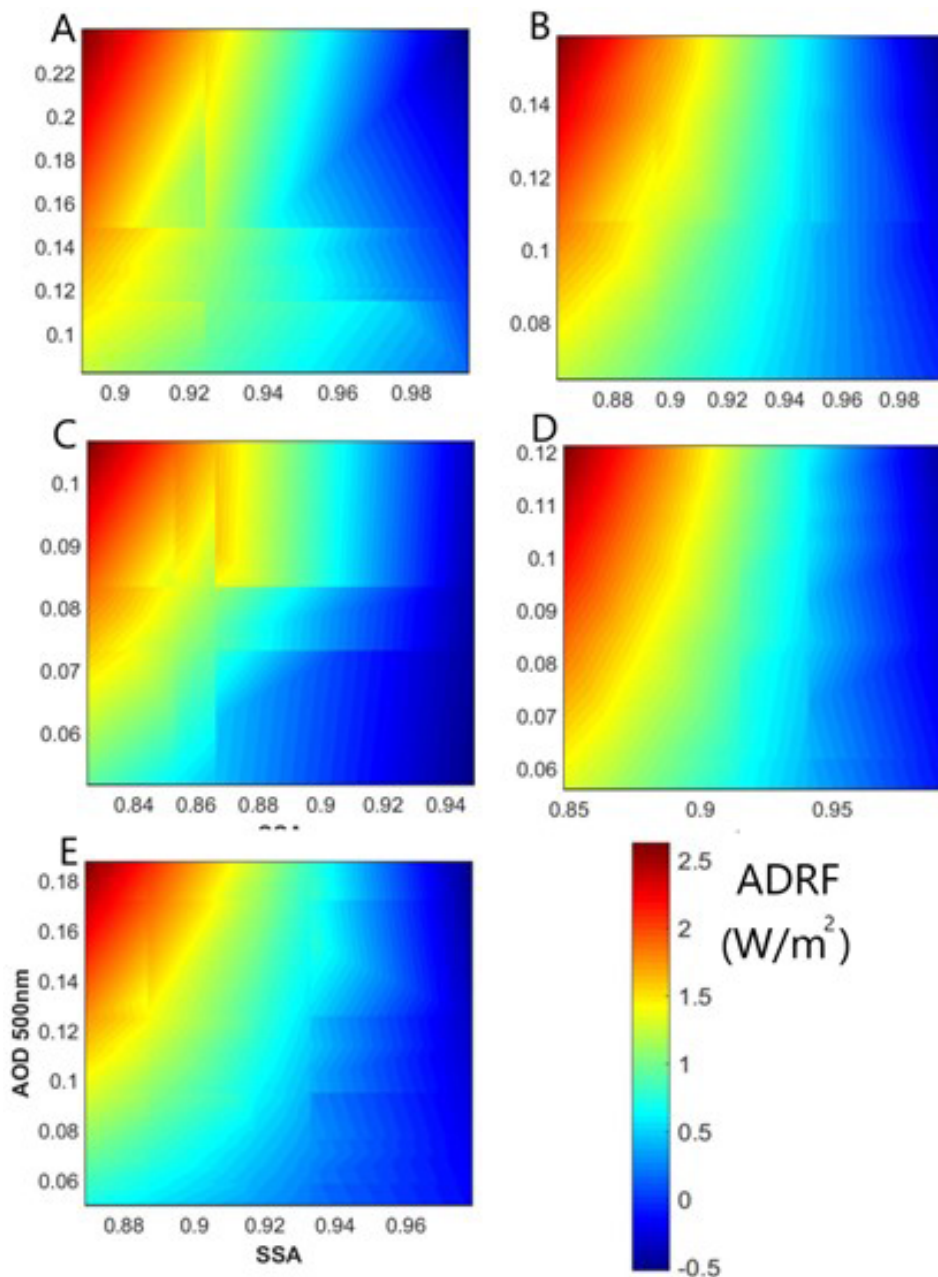


**Figure 7** Dependence of single scattering albedo ( $\omega$ ) and AOD on the direct aerosol radiative forcing for OH in 2022 in the: A. April; B. May; C. June; D. July; E. August.



## 4 Discussion of Results

Atmospheric particles (PM<sub>10</sub> and PM<sub>2.5</sub>) are responsible for serious problems in human health. For this reason, PM<sub>10</sub> and PM<sub>2.5</sub> exceed the Environmental Quality Standard for Air of Peruvian legislation, for both particle sizes.

In total, five emission sources have been detected for the urban sites of the Mantaro Valley: soil dust (Al, Ca, Si, Fe, Ti, Mn and K), biomass burning (Cl, Br, K), vehicles (Cu, Zn, Cl, Cr), fuel-oil (Ni) and foundry (Pb, Zn, As and Cu), with soil dust being the main source of PM<sub>10</sub> and PM<sub>2.5</sub> (Álvarez-Tolentino & Suárez-Salas 2020).

The PM<sub>2.5</sub> concentration in Huancayo was  $17.1 \pm 5.15 \mu\text{g}/\text{m}^3$  (Lizarraga-Isla et al. 2019). On the other hand, the mean annual concentration of PM<sub>2.5</sub> in Huancayo has ranged (average) from 3.4 to  $36.8 \mu\text{g}/\text{m}^3$  ( $16.6 \pm 6.8 \mu\text{g}/\text{m}^3$ ) and exceeded the annual thresholds of the Organization World Health Organization and national air quality standards (De La Cruz et al. 2019).

The influence of PM<sub>10</sub> particles on the optical thickness of aerosols in the central Andes of Peru, the results showed an increase in PM<sub>10</sub> concentrations with an increase in the number of fire outbreaks and in the AOD during July, August and September. In contrast, in October there was a slight decrease in PM<sub>10</sub> concentrations. In addition, the meteorological conditions did not favor the occurrence of fire outbreaks in the Mantaro Valley during the entire study period; however, an increase in precipitation reduced aerosol concentrations in October. Although the vertical movements that prevailed over the central Andes were ascending, they descended along the Peruvian coast, favoring and hindering the dispersion of aerosols (Navarro-Barboza et al. 2020).

On the other hand, studies that used the same methodology to estimate air quality during the COVID-19 pandemic, such as in Rio de Janeiro, air quality was classified as “good”. Brazilian air quality standards for SO<sub>2</sub>, O<sub>3</sub>, and NO<sub>2</sub> were not exceeded at any of the monitoring stations during the partial shutdown due to COVID-19. Also note that the improvements in air quality during the partial closure due to COVID-19 can be mainly attributed to a reduction in emission sources rather than weather conditions (Beringui et al. 2023). Also note that during the COVID-19 pandemic, the partial closure contributed to improving air quality in the city of Rio de Janeiro, which means that changes in the work format can be an alternative to reduce air pollution in large cities, since the home office contributes to the reduction of mobility and, consequently, to vehicle emissions (Beringui et al. 2022).

## 5 Conclusions

Measurements of optical properties of aerosols performed during dry season 2022. During this period, values of AOD (500 nm) varied between 0.06 to 0.22, presented value maximum that is 0.24 (April) and minimum that is 0.05 (June).

The Angstrom coefficient shows the mean value for Angstrom coefficient ( $\alpha$ ) varied from 0.03 to 1.6 (April). Also, average monthly values of the aerosol volume-size distribution maximum values correspond to the coarse mode (radius < 10  $\mu\text{m}$ ). They can be found between the months of April and August with magnitudes higher than  $0.06 \mu\text{m}^3 / \mu\text{m}^2$  and correspond to the coarse mode.

The daily average values of PM<sub>2.5</sub> and PM<sub>10</sub> are compared with the Environmental Quality Standards of the Peruvian Regulations ( $50 \mu\text{g}/\text{m}^3$  and  $100 \mu\text{g}/\text{m}^3$ ), where it is determined that they are not exceeded. Nevertheless, the AQI was calculated for PM<sub>2.5</sub>, and PM<sub>10</sub> during April - August 2022, presented AQI values classified as “good” and “moderate. Also, recorded optical properties were used to estimate ARDF at the top of the atmosphere. The results indicate that the ARDF is between  $[-0.5 \ 2.5] \text{W}/\text{m}^2$ .

The development of a low-cost sensors represents a potential alternative that can complement reference air quality monitor stations worldwide because of the low cost and minimal maintenance requirements during operation (Romero, Velásquez & Noel 2020).

The study allows us to indicate the state of air quality in Huancayo from the levels of pollution of PM<sub>2.5</sub> and PM<sub>10</sub>. Therefore, any planning strategy aimed at reducing air pollution must consider its current state of development and, based on which, design its future plan.

With the present investigation, continuous monitoring of atmospheric particles, for this reason it is necessary to implement air quality management measures for the Mantaro valley

## 6 Acknowledgments

Thanks to NASA Aeronet Program for making the data available.

## 7 References

Álvarez-Tolentino, D. & Suárez-Salas, L. 2020, ‘Aporte cuantitativo de las fuentes de PM<sub>10</sub> Y PM<sub>2.5</sub> en sitios urbanos Del Valle Del Mantaro, Perú’, *Revista Internacional de Contaminación Ambiental*, vol. 36, no. 4, pp. 875-92, DOI:10.20937/RICA.53473.

- Ardon-Dryer, K., Dryer, Y., Williams, J.N. & Moghimi, N. 2020, 'Measurements of PM<sub>2.5</sub> with PurpleAir under atmospheric conditions', *Atmospheric Measurement Techniques*, vol. 13, no. 10, pp. 5441-58, DOI:10.5194/amt-13-5441-2020.
- Bedareva, T.V., Sviridenkov, M.A. & Zhuravleva, T.B. 2014, 'Retrieval of dust aerosol optical and microphysical properties from ground-based Sun-sky radiometer measurements in approximation of randomly oriented spheroids', *Journal of Quantitative Spectroscopy and Radiative Transfer*, vol. 146, pp. 140-57, DOI:10.1016/j.jqsrt.2014.05.006.
- Beringui, K., Justo, E., Ventura, L., Gomes, R., Lionel-Mateus, V., De La Cruz, A., de Almeida, A.C., Ramos, M., Angeles Suazo, J., Valle, P. & Gioda, A. 2023, 'The contribution of meteorological parameters and the COVID-19 partial lockdown on air quality in Rio de Janeiro, Brazil', *Journal of the Brazilian Chemical Society*, vol. 34, no. 1, pp. 69-82, DOI:10.21577/0103-5053.20220089.
- Beringui, K., Justo, E.P.S., De Falco, A., Santa-Helena, E., Rocha, W.F.C., Deroubaix, A. & Gioda, A. 2022, 'Assessment of air quality changes during COVID-19 partial lockdown in a Brazilian metropolis: From lockdown to economic opening of Rio de Janeiro, Brazil', *Air Quality, Atmosphere and Health*, vol. 15, no. 7, pp. 1205-20, DOI:10.1007/s11869-021-01127-2.
- Castro, T., Madronich, S., Rivale, S., Muhlia, A. & Mar, B. 2001, 'The influence of aerosols on photochemical smog in Mexico City', *Atmospheric Environment*, vol. 35, no. 10, pp. 1765-72, DOI:10.1016/S1352-2310(00)00449-0.
- Charlson, R.J., Schwartz, S.E., Hales, J.M., Cess, R.D., Coakley, J.A., Hansen, J.E. & Hofmann, D.J. 1992, 'Climate forcing by anthropogenic aerosols', *Science*, vol. 255, no. 5043, pp. 423-30, DOI:10.1126/science.255.5043.423.
- Chýlek, P., Videen, G., Geldart, D.J.W., Dobbie, J.S. & Tso, H.C.W. 2000, 'Effective Medium approximations for Heterogeneous Particles', *Light Scattering by Nonspherical Particles*, DOI:10.1016/B978-12498660-2/50036-7.
- De La Cruz, A.H., Roca, Y.B., Suarez-Salas, L., Pomalaya, J., Tolentino, D.A. & Gioda, A. 2019, 'Chemical characterization of PM<sub>2.5</sub> at rural and urban sites around the metropolitan area of Huancayo (Central Andes of Peru)', *Atmosphere*, vol. 10, no. 21, 21, DOI:10.3390/atmos10010021.
- Dubovik, O. & King, M.D. 2000, 'A flexible inversion algorithm for retrieval of aerosol optical properties from Sun and sky radiance measurements', *Journal of Geophysical Research Atmospheres*, vol. 105, no. D16, pp. 673-96, DOI:10.1029/2000JD900282.
- Eck, T.F., Holben, B.N., Reid, J.S., Dubovik, O., Smirnov, A., O'Neill, N.T., Slutsker, I. & Kinne, S. 1999, 'Wavelength dependence of the optical depth of biomass burning, urban, and desert dust aerosols', *Journal of Geophysical Research Atmospheres*, vol. 104, no. D24, pp. 333-49.
- Eck, T.F., Holben, B.N., Reid, J.S., O'Neill, N.T., Schafer, J.S., Dubovik, O., Smirnov, A., Yamasoe, M.A. & Artaxo, P. 2003, 'High aerosol optical depth biomass burning events: A comparison of optical properties for different source regions', *Geophysical Research Letters*, vol. 30, no. 20, pp. 1-4, DOI:10.1029/2003GL017861.
- Estevan, R., Martínez-Castro, D., Suarez-Salas, L., Moya, A. & Silva, Y. 2019, 'First two and a half years of aerosol measurements with an AERONET sunphotometer at the Huancayo Observatory, Peru', *Atmospheric Environment: X*, vol. X, no. 3, 100037, DOI:10.1016/j.aeoa.2019.100037.
- Forster, P., Ramaswamy, V., Artaxo, P., Berntsen, T., Betts, R., Fahey, D.W., Haywood, J., Lean, J., Lowe, D.C., Myhre, G., Nganga, J., Prinn, R., Raga, G., Schulz, M. & Van Dorland, R. 2010, 'Changes in Atmospheric Constituents and in Radiative Forcing Coordinating', in S. Solomons, D. Qin, M. Manning, Z. Chen, M. Marquis, K.B. Averyt, M. Tignor & H.L. Miller (eds) *Climate change 2007: The physical science basis, contribution of working group I to the fourth Assessment Report of the Intergovernmental Panel on Climate Change*, Cambridge University Press, Cambridge, pp. 131-217.
- Gobbi, G.P., Kaufman, Y.J., Koren, I. & Eck, T.F. 2007, 'Classification of aerosol properties derived from AERONET direct sun data', *Atmospheric Chemistry and Physics*, vol. 7, no. 2, pp. 453-8.
- Habib, A., Chen, B., Khalid, B., Tan, S., Che, H., Mahmood, T., Shi, G. & Butt, M.T. 2019, 'Estimation and inter-comparison of dust aerosols based on MODIS, MISR and AERONET retrievals over Asian desert regions', *Journal of Environmental Sciences (China)*, vol. 76, pp. 154-66, DOI:10.1016/j.jes.2018.04.019.
- Haywood, J. & Boucher, O. 2000, 'Estimates of the direct and indirect radiative forcing due to tropospheric aerosols: A review', *Reviews of Geophysics*, vol. 38, no. 4, pp. 513-43, DOI:10.1029/1999RG000078.
- Haywood, J.M. & Shine, K.P. 1995, 'The effect of anthropogenic sulfate and soot aerosol on the clear sky planetary radiation budget', *Geophysical Research Letters*, vol. 22, no. 5, pp. 603-6, DOI:10.1029/95GL00075.
- Holben, B.N., Eck, T.F., Slutsker, I., Smirnov, A., Sinyuk, A., Schafer, J., Giles, D. & Dubovik, O. 2006, 'Aeronet's Version 2.0 quality assurance criteria', *Remote Sensing of the Atmosphere and Clouds*, vol. 6408, 64080Q, DOI:10.1117/12.706524.
- Holben, B.N., Eck, T.F., Slutsker, I., Tanré, D., Buis, J.P., Setzer, A., Vermote, E., Reagan, J.A., Kaufman, Y.J., Nakajima, T., Lavenu, F., Jankowiak, I. & Smirnov, A. 1998, AERONET – a federated instrument network and data archive for aerosol characterization, *Remote Sensing of Environment*, vol. 66, no. 1, pp. 1-16, DOI:10.1016/S0034-4257(98)00031-5.
- IPCC – Intergovernmental Panel on Climate Change 2007, 'Climate Change 2007: The Physical Science Basis. Contribution of Working Group I to the Fourth Assessment Report of the Intergovernmental Panel on Climate Change. Summary for Policymakers', *Climate Change 2007: The Physical Science Basis. Contribution of Working Group I to the Fourth Assessment Report of the Intergovernmental Panel on Climate Change*.
- Kuttippurath, J. & Raj, S. 2021, 'Two decades of aerosol observations by AATSR, MISR, MODIS and MERRA-2 over India and Indian Ocean', *Remote Sensing of Environment*, vol. 257, 112363, DOI:10.1016/j.rse.2021.112363.
- Lizarraga-Isla, I.J., Pomalaya-Valdez, J.E., Suarez-Salas, L.F. & Bendezu-Roca, Y. 2019, 'Dispersion of particulate material 2.5 emitted by roasted chicken restaurants using the aermod

- model in huancayo metropolitan, Peru', *DYNA*, vol. 86, no. 211, pp. 346-53, DOI:10.15446/dyna.v86n211.78812.
- Masson-Delmotte, V., Zhai, P., Pirani, A., Connors, S.L., Péan, C., Berger, S., Caud, N., Chen, Y., Goldfarb, L., Gomis, M.I., Huang, M., Leitzell, K., Lonnoy, E., Matthews, J.B.R., Maycock, T.K., Waterfield, T., Yelekçi, O., Yu, R. & Zhou, B. (eds) 2021, *IPCC, 2021: Climate Change 2021: The Physical Science Basis*, Cambridge University Press.
- Navarro-Barboza, H., Moya-Álvarez, A., Luna, A. & Fashé-Raymundo, O. 2020, 'Influence evaluation of PM10 produced by the burning of biomass in Peru on AOD, using the WRF-Chem', *Atmosfera*, vol. 33, no. 1, pp. 71-86, DOI:10.20937/atm.52711.
- Olcese, L.E., Palancar, G.G. & Toselli, B.M. 2014, 'Aerosol optical properties in central Argentina', *Journal of Aerosol Science*, vol. 68, pp. 25-37, DOI:10.1016/j.jaerosci.2013.11.003.
- Otero, L., Ristori, P., Holben, B. & Quel, E. 2006, 'Espesor óptico de aerosoles durante el año 2002 para diez estaciones pertenecientes a la red AERONET-NASA' *Óptica Pura y Aplicada*, vol. 39, no. 4, pp. 355-64.
- Romero, Y., Velásquez, R.M.A. & Noel, J. 2020, 'Development of a multiple regression model to calibrate a low-cost sensor considering reference measurements and meteorological parameters', *Environmental Monitoring and Assessment*, vol. 192, no. 8, 498, DOI:10.1007/s10661-020-08440-w.
- Sayahi, T., Kaufman, D., Becnel, T., Kaur, K., Butterfield, A.E., Collingwood, S., Zhang, Y., Gaillardon, P.-E. & Kelly, K.E. 2019, 'Development of a calibration chamber to evaluate the performance of low-cost particulate matter sensors', *Environmental Pollution*, vol. 255, no. 1, 113131, DOI:10.1016/j.envpol.2019.113131.
- Shifrin, K.S. 1995, 'Simple relationships for the Ångström parameter of disperse systems', *Applied Optics*, vol. 34, no. 21, pp. 4480-5, DOI:10.1364/AO.34.004480.
- Srivastava, A.K., Singh, S., Tiwari, S. & Bisht, D.S. 2012, 'Contribution of anthropogenic aerosols in direct radiative forcing and atmospheric heating rate over Delhi in the Indo-Gangetic Basin', *Environmental Science and Pollution Research*, vol. 19, no. 4, pp. 1144-58, DOI:10.1007/s11356-011-0633-y.
- Suazo, J.M.A., Salas, L.S., Cruz, A.R.H.D., La Vasquez, R.A., Aylas, G.R., Condor, A.R., Rojas, E.R., Ccuro, F.M., Rojas, J.L.F. & Karam, H.A. 2020, 'Direct radiative forcing due to aerosol properties at the peruvian antarctic station and metropolitan huancayo area', *Anuario do Instituto de Geociências*, vol. 43, no. 4, pp. 404-12, DOI:10.11137/2020\_4\_404\_412.

#### Author contributions

**Roberto Angeles Vasquez:** conceptualization; formal analysis; methodology; writing-original draft; writing – review and editing; visualization; conceptual discussions. **Julio Angeles Suazo:** conceptualization; formal analysis; methodology; writing-original draft; validation; conceptual discussions. **Hugo Abi Karam:** formal conceptual analysis; conceptual discussions. **Jose Luis Flores Rojas:** conceptual discussions. **Luis Suarez Salas:** formal conceptual analysis; conceptual discussions. **Carmencita Lavado Meza:** conceptual discussions. **Nataly Angeles Suazo:** conceptual discussions. **Fernando Boza Ccora:** conceptual discussions. **Leonel de la Cruz Cerron:** conceptual discussions. **Rosa Zarate Quiñones:** conceptual discussions.

#### Conflict of interest

The authors declare no conflict of interest.

#### How to cite:

Angeles Vasquez, R., Suazo, J.M.A., Karam, H.A., Flores Rojas, J.L., Suarez Salas, L., Lavado-Meza, C., Angeles Suazo, N., Boza Ccora, F., De la Cruz-Cerron, L. & Zarate Quiñones, R. 2024, 'Atmospheric Aerosols and Air Quality in the 2022 Dry Season in Huancayo-Perú', *Anuário do Instituto de Geociências*, 47:56253. [https://doi.org/10.11137/1982-3908\\_2024\\_47\\_56253](https://doi.org/10.11137/1982-3908_2024_47_56253)

#### Data availability statement

Reference datasets, scripts and code are available on request.

#### Funding information

Not applicable.

#### Editor-in-chief

Dr. Claudine Dereczynski

#### Associate Editor

Dr. Gerson Cardoso da Silva Jr.

